

Laser spectroscopy of the HgZn excimer

J. Supronowicz, E. Hegazi, G. Chambaud,* J. B. Atkinson, W. E. Baylis, and L. Krause
Department of Physics, University of Windsor, Windsor, Ontario, Canada N9B3P4

(Received 27 August 1987)

Extensive and previously unknown fluorescence and excitation spectra of the HgZn excimer have been observed and correlated with a potential-energy (PE) diagram. The spectra were excited in a Hg-Zn mixture contained in a quartz vapor cell by successive pulses from two dye lasers, using the pump-and-probe methods, and the PE curves were derived from Hg and Zn atomic parameters, previously known Hg₂ and Zn₂ curves, and from molecular-orbital considerations. There is good agreement between the measured and calculated transition energies.

INTRODUCTION

There have been several recent reports on experimental and theoretical studies of group-2b metallic excimers, which exhibit spectral emission in the blue-green spectral region and might become vehicles for molecular dissociation lasers.¹ Of particular interest are the spectroscopic investigations of Hg₂ (Refs. 2 and 3) and Hg₃,⁴ the calculations of potential-energy (PE) curves for Hg₂ and TlHg,⁵ and of the energy levels of Zn₂ (Ref. 6) and Zn₃.⁷ The many efforts to produce lasers based on transitions in the blue-green region in Hg₂, HgCd, or HgTl excimers have not met with success, probably because of too many absorption processes competing with the stimulated emission. In the HgZn excimer, only one broad emission band was observed at 460 nm, arising from a transition from an excited HgZn state to the dissociative ground state.⁸ We now report the preliminary results of an extensive experimental and theoretical investigation of HgZn, in which we observed several fluorescence and excitation bands and assigned them to transitions between specific molecular states located on a PE diagram which was produced simultaneously but independently of the experimental study.

POTENTIAL-ENERGY CURVES

A schematic representation of the PE curves shown in Fig. 1 has been derived from Hg and Zn atomic parameters⁹ and from PE curves of Hg₂ (Refs. 5, 10, and 11) and Zn₂.^{7,12,13} The X¹Σ ground state is the average of the Hg₂ and Zn₂ ground states, with the same asymptotic energy which is also taken as a reference zero value for the higher PE curves whose asymptotic values were assumed from experimental data.⁹ For the sake of simplicity and clarity, the potential curves are drawn and labeled according to Hund's case-*a* coupling, where spin-orbit effects are taken to be small. In view of the large fine-structure splitting in atomic mercury, this is a rather poor approximation, and it would be more appropriate to use Hund's case-*c* coupling, in which the curves are labeled by Ω, the quantum number corresponding to the projection of the electronic angular momentum *j* on the internuclear axis, and in which curves of the same Ω do not cross. The *c*-case curves can be estimated first by splitting the case-*a* curves

into different *j* components with $|L-S| \leq j \leq L+S$ with splittings intermediate between those of Hg (³*P*) and those of Zn (³*P*), and then by dividing these further into curves of differing Ω ($|\Lambda-\Sigma| \leq \Omega \leq \Lambda+\Sigma$) and replacing crossings of curves with like Ω by anticrossings whose minimum separations are also of the order of the atomic fine-structure splittings. Thus, for example, a curve labeled ³Π on our diagram splits into four curves in case-*c* coupling: Two with Ω=0, one with Ω=1, and one with Ω=2. In Hund's case *a*, the low-lying excited states arise from three groups of states that are combined into a PE diagram which also includes the appropriate avoided crossings.

The first group of states is formed from a ground-state Hg or Zn atom and the other atom in a ³*P* or ¹*P* excited state, corresponding to the configurations *ns, np*. Considerations of molecular-orbital energy levels indicate that the lowest excited states, correlated with the Zn (³*P*) state, should have a (binding) character similar to the ³Σ_u⁺ and ³Π_g states of Zn₂, except that in HgZn the bond is longer and the PE well depth smaller than in Zn₂. Simi-

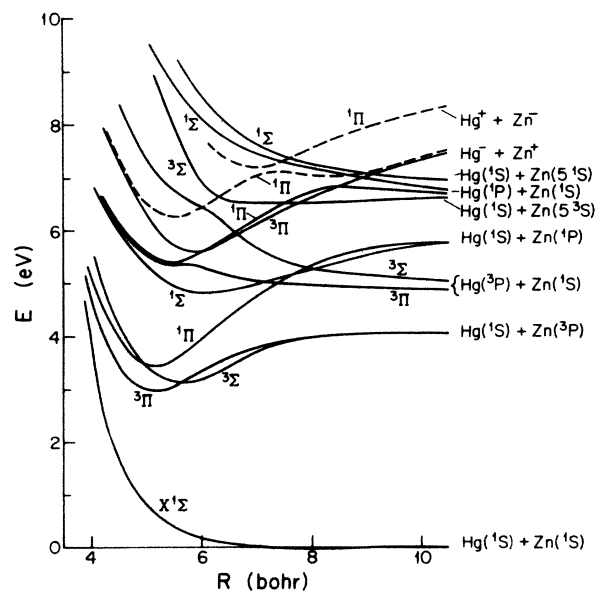


FIG. 1. PE diagram showing low-lying HgZn states.

lar arguments apply to the states $^1\Pi$ and $^1\Sigma$ correlated with the Zn 1P state, and it is possible to deduce that the states correlated with the Hg ($^3P, ^1P$) atomic states are repulsive, though less than in the case of Hg₂.

The second group arises from ionic states of which the lowest corresponds to Hg⁻ + Zn⁺. Since the ionization potential of Zn (9.39 eV) is lower than that of Hg (10.43 eV) and the "electron affinities" of Hg and Zn are about -0.6 and -0.5 eV, respectively,¹⁴ the $^1\Pi$ ionic states interact strongly with repulsive states correlated with Zn (1S) + Hg ($^1P, ^3P$), producing an avoided crossing with the $^1\Pi$ state (Zn 1S + Hg 1P), and a deep well. There is also an avoided crossing of the ionic $^3\Pi$ state with a repulsive $^3\Pi$ state (Zn 1S + Hg 3P) at a smaller internuclear separation (about 6 bohr), which produces a shallow well. The ionic states corresponding to Hg⁺ + Zn⁻ are less important since they have higher energies and do not interact directly with the first group of states.

The third group is derived from ground-state Hg and excited Zn in the configuration ($4s, 5s$)^{1,3}S. Although no previous Zn₂ data are available, we can reasonably assume that the $^3\Sigma$ state (Hg 1S + Zn 5^3S) is not strongly bound and that the $^1\Sigma$ state (Hg 1S + Zn 5^1S) is not very repulsive; avoided crossings can occur between these states and those of the first group.

THE APPARATUS AND EXPERIMENTAL PROCEDURE

The apparatus and procedures employed in the pump-and-probe experiments have been described previously.¹⁵ A mixture of Hg and Zn vapor contained in a quartz cell was irradiated with two successive ("pump" and "probe") dye-laser pulses. The resulting fluorescence, observed at right angles to the direction of excitation, was resolved with a monochromator, detected with a photomultiplier, and registered with a transient digitizer whose output was integrated and analyzed in a microcomputer, which also scanned the probe laser and monochromator. The pump pulse was produced in a two-stage dye laser operated with Rh 640 dye and excited with the second harmonic (532 nm) of a Q-switched Nd:YAG laser (where YAG is yttrium aluminum garnet). The resulting output at 615.2 nm was frequency doubled to produce 8-ns pulses of 307.59 nm radiation corresponding to the $4^3P_1 \leftarrow 4^1S_0$ Zn intercombination line, which were weakly focused in the vapor cell. When appropriate, the irradiated region was probed after a 450-ns delay with a second pulse from a N₂-laser-pumped dye laser directed collinearly with the pump pulse, whose half-width was about 8 ns and spectral linewidth about 0.3 cm⁻¹. The sealed fluorescence cell was fitted with a side arm and was mounted in an oven which maintained the cell at about 840 K and the side arm at about 780 K.

The experiment was carried out in three separate but mutually complementary stages. The first stage dealt with the HgZn fluorescence produced by the pump pulse only, which consisted of the previously observed⁸ blue band and whose time evolution was recorded at various vapor densities. At the same time, the spectral profile of this band was studied as well as the time evolution of the

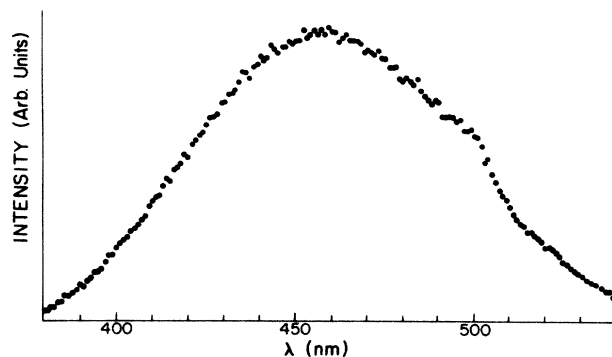


FIG. 2. A trace of the fluorescence band excited with 307.56 nm laser radiation.

307.6 nm atomic Zn fluorescence. The second stage involved pump-and-probe experiments at a constant cell temperature, with monochromator scans of the fluorescence spectrum. The pump-probe delay was set at 450 ns which corresponded to the maximal intensity of the blue band and the profile of the resulting fluorescence band near 250 nm was recorded as described previously.¹⁵ In the third stage of the experiment, the monochromator setting was fixed and the probe laser was scanned, producing excitation spectra. The scanning increment was 0.2–0.3 nm and the resulting excitation spectra appear to exhibit a regular structure, typical of vibrational excitation bands.²

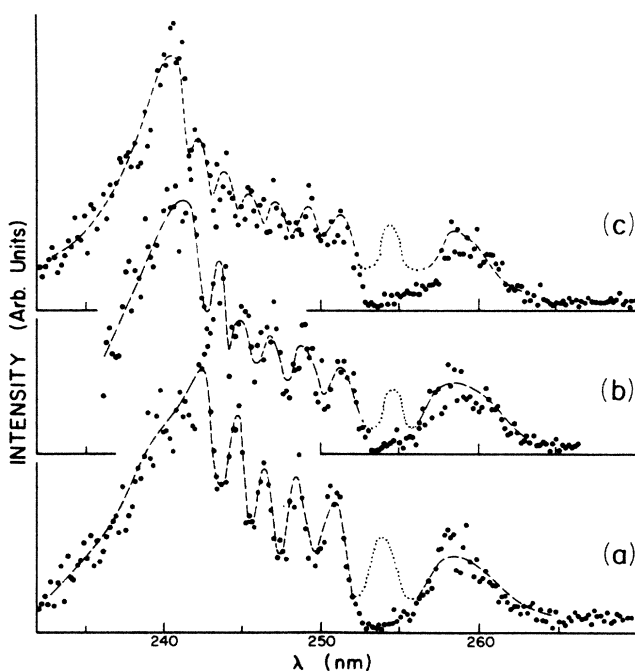


FIG. 3. LIF bands emitted from selectively populated v' states. (a) $v' = 6$; (b) $v' = 7$; (c) $v' = 8$. The wavelengths of the probe radiation were (a) 566.0 nm; (b) 562.0 nm; (c) 558.8 nm. The dashed lines suggest the spectral profiles, the dotted lines indicate the position of the components absorbed by Hg.

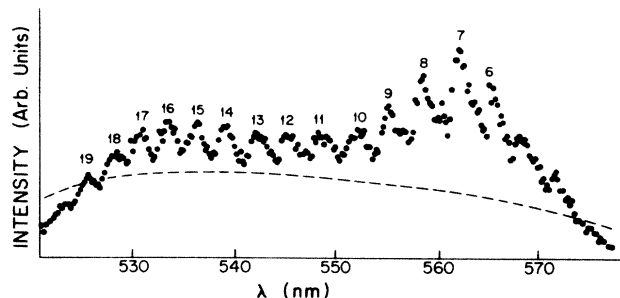


FIG. 4. Partial ${}^1\Pi \leftarrow {}^1\Pi$ excitation spectrum showing v' assignments ($v''=0$). The dashed curve indicates relative dye laser output power.

EXPERIMENTAL RESULTS AND DISCUSSION

Figure 2 shows the spectral profile of the 460 nm fluorescence band excited with the pump laser. As already reported, the band peaks at about 460 nm, but the additional component on its shoulder near 500 nm had not been previously observed.⁸ We believe the 460 nm band to arise from the ${}^3\Sigma(\text{Hg } {}^1S + \text{Zn } {}^3P) \rightarrow X{}^1\Sigma$ decay and ascribe the 500 nm component to the ${}^1\Pi(\text{Hg } {}^1S + \text{Zn } {}^1P) \rightarrow X{}^1\Sigma$ transition. We also registered the time evolution of the 460 nm fluorescence following the pump pulse and found that, after a relatively fast rise, the band intensity reaches a maximum and decays exponentially as a slower rate, with a decay time of 6 μs . Although the specific rise and decay times depend on the vapor density in the cell, we found the rise time of the band fluorescence to be equal to the decay time of the atomic 307.59 nm fluorescence, which confirms the suggested mechanism⁸ for the formation of HgZn:



the efficiency of this process appears to be quite high. The presence of the reactive collisions shortens the effective lifetime of Zn (4^3P_1) atoms by about two orders of magnitude, in keeping with Eden's observations.⁸ On the other hand, the HgZn excimer appears to be relatively insensitive to quenching by Hg collisions, even at Hg vapor pressures above 1 atm.

Figure 3 shows a series of laser-induced-fluorescence (LIF) spectra, representing the bound-free decays of vibrational states selectively populated using pump and probe excitation. These are representative "Condon internal diffraction" patterns centered near 250 nm, similar to those observed with Hg₂.¹⁵ It is unfortunate that the bands are partly obscured by the strong Hg absorption line at 253.7 nm. The LIF spectra are due to the

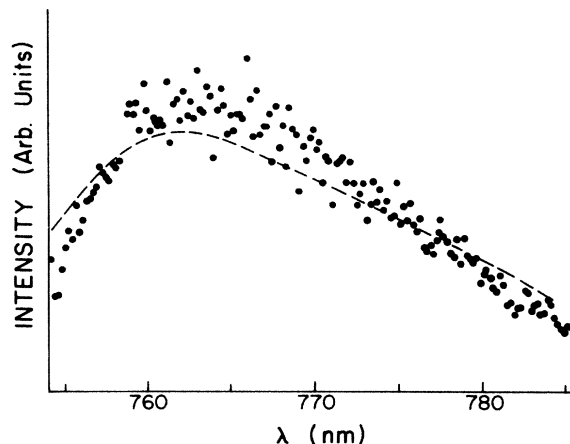


FIG. 5. Partial ${}^1\Sigma \leftarrow {}^3\Sigma$ excitation spectrum. The dashed curve indicates relative dye laser output power.

${}^1\Pi(\text{Hg } {}^1P, \text{Zn } {}^1S) \rightarrow X{}^1\Sigma$ decays.

The excitation band shown in Fig. 4 is part of a very broad spectrum extending from 500–660 nm, which was recorded with the monochromator set at 242 nm. Some of the clearly resolved vibrational components, forming a v' progression, have been identified by a comparison of the excitation and bound-free fluorescence spectra shown in Fig. 3. We interpret this spectrum to be due to the ${}^1\Pi(\text{Hg } {}^1P, \text{Zn } {}^1S) \leftarrow {}^1\Pi(\text{Hg } {}^1S, \text{Zn } {}^1P)$ absorption, assuming the latter state to be populated through the ${}^3\Sigma$ - ${}^1\Pi$ curve crossing.

We have observed an additional excitation spectrum extending from 640–790 nm, which possesses a rich and complex vibrational structure, not yet properly resolved or analyzed. A part of this spectrum (which was recorded at 275.1 nm) is shown in Fig. 5 and the band is ascribed to the ${}^1\Sigma(\text{Hg } {}^1S, \text{Zn } {}^1P) \leftarrow {}^3\Sigma(\text{Hg } {}^1S, \text{Zn } {}^3P)$ absorption.

There is a gratifying degree of agreement between the measured wavelengths of the various fluorescence and excitation bands and those predicted by the PE diagram. The assignments of the excitation spectra should be regarded as provisional since we do not know yet whether the probe excitation takes place from the ${}^3\Sigma(\text{Hg } {}^1S + \text{Zn } {}^3P)$ state or from another reservoir state nearby.

ACKNOWLEDGMENTS

This research was supported by a grant from the Natural Sciences and Engineering Research Council of Canada. One of us (G. C.) has participated in this research under the auspices of the Program of Scientific and Technological Cooperation Canada-France.

*Permanent Address: Laboratoire de Physico Chimie des Rayonnements, University of Paris XI, Orsay, France.

¹G. Rodriguez, K. P. Killeen, and J. G. Eden, International Laser Science Conference, 1986, Technical Digest (unpub-

lished).

²R. J. Niefer, J. Supronowicz, J. B. Atkinson, and L. Krause, Phys. Rev. A **35**, 4629 (1987), and references within.

³A. B. Callear, Chem. Rev. **87**, 335 (1987).

- ⁴R. J. Niefer, J. Supronowicz, J. B. Atkinson, and L. Krause, *Phys. Rev. A* **34**, 2483 (1986).
- ⁵K. C. Celestino and W. C. Ermler, *J. Chem. Phys.* **81**, 1872 (1984).
- ⁶C. H. Su, Y. Huang, and R. F. Brebrick, *J. Phys. B* **18**, 3187 (1985).
- ⁷H. Tatewaki, M. Tomonari, and T. Nakamura, *J. Chem. Phys.* **82**, 5608 (1985).
- ⁸J. G. Eden, *Opt. Commun.* **25**, 201 (1978).
- ⁹C. E. Moore, *Natl. Bur. Stand. U.S.A. Circ. No. 467*, Vol. III (1958).
- ¹⁰W. E. Baylis, *J. Phys. B* **10**, L583 (1977).
- ¹¹F. H. Mies, W. J. Stevens, and M. Krauss, *J. Mol. Spectrosc.* **72**, 303 (1978).
- ¹²P. J. Hay, T. H. Dunning, and R. C. Raffanetti, *J. Chem. Phys.* **65**, 2679 (1976).
- ¹³C. F. Bender, T. N. Rescigno, H. F. Schaefer III, and A. E. Orel, *J. Chem. Phys.* **71**, 1122 (1979).
- ¹⁴The ions Zn^- and Hg^- are not stable, but their ground states appear as sharp resonances in electron scattering. See P. D. Burrow, J. A. Michejda, and T. Comer, *J. Phys. B* **9**, 3225 (1976).
- ¹⁵R. J. Niefer, J. Supronowicz, J. B. Atkinson, and L. Krause, *Phys. Rev. A* **34**, 1137 (1986).